Matrix Methods for Microstrip Three-Dimensional Problems

ANDREW FARRAR, MEMBER, IEEE, AND ARLON TAYLOR ADAMS, MEMBER, IEEE

Abstract—The matrix methods are applied to three-dimensional microstrip problems with emphasis upon the general problem of discontinuities in microstrip. Discontinuities considered are 1) open circuits, 2) change of width, and 3) gap in microstrip. Also, the capacitance of rectangular sections of microstrip is computed. Computed data agree well with experiment and data in the literature.

I. Introduction

THE METHOD of matrix inversion has been used previously in solving scattering and radiation problems in electromagnetic field theory [1]–[3]. Recently, the method has been applied to some two-dimensional and three-dimensional problems in microstrip [4], [5]. Discontinuities such as a step or a gap in the center conductor of microstrip constitute three-dimensional problems. This paper describes the application of the matrix methods to three-dimensional microstrip problems, with particular emphasis upon the general problem of discontinuities in microstrip. Determination of the equivalent circuit parameters of a discontinuity, generally known as the characterization data, is an important and necessary step in developing computer-aided network-design techniques for microstrip. Only limited amounts of theoretical or experimental data [6] on discontinuities in (inhomogeneous) microstrip have been reported, although there is extensive data on (homogeneous) balanced strip transmission-line [7] and coaxial-line [8] discontinuities.

The purpose of this paper is twofold; first, to describe the formulation of microstrip discontinuity problems in terms of the matrix inversion method, and second, to illustrate the use of this formalism by its application to several microstrip discontinuities. The discontinuities treated here are open circuits, gaps, and sudden change of width. Data are plotted for a few commonly used dielectric constants ($\epsilon_r = 1.0$, 6.0, 9.6) and some comparison is made with available theoretical and experimental data. The method outlined is a general one and is applicable to any discontinuity: to obtain the excess or lumped capacitance of a one-port device or the excess or lumped static-capacitance matrix of an N-port device.

Manuscript received July 29, 1971; revised October 10, 1971. This research was supported in part by the Rome Air Development Center, Griffiss Air Force Base, under Contract AF30(602)2636, and was pursued under Rome Air Development Center Post Doctoral Program in cooperation with Syracuse University under Contract F30602-68-C-0086.

A. Farrar is with the Heavy Military Electronic Systems, General Electric Company, Syracuse, N. Y.

A. T. Adams is with the Department of Electrical Engineering, Syracuse University, Syracuse, N. Y. 13210.

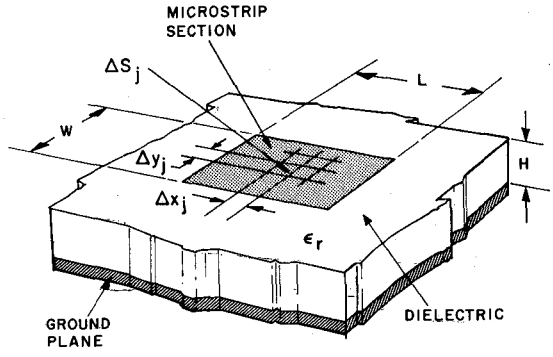

Fig. 1. Microstrip rectangular section.

II. Matrix Methods for Three-Dimensional Problems

A. Finite Three-Dimensional Problems—Rectangular Sections of Microstrip

The matrix method is a technique that reduces the defining integral equation to an approximate matrix equation. The formulation of the three-dimensional problem is similar to that for the two-dimensional problem except that a new three-dimensional source function (or integral of a Green's function) is required. The basic three-dimensional source function, i.e., the potential due to a uniformly charged rectangular section in microstrip, is given in the Appendix. In this section, we consider first three-dimensional problems of finite extent, and the specific example of rectangular sections of microstrip (a pad) is treated. Next, the discontinuity problem, which is essentially a problem of infinite extent, is considered and several specific examples are given.

A rectangular section of microstrip transmission line, of length L, width W, and height H above the ground plane, is shown in Fig. 1. The rectangular surface is subdivided into n subsections. We assume that the charge density is constant over each subsection (pulse expansion functions) [1]. Let σ_j be the surface charge density over Δs_j. Point matching (impulsive weights) [1] is used. The basic three-dimensional source function D_{ij} (the potential at point i due to a uniformly charged subsection Δs), with a unit charge density, is given in the Appendix. The ground plane is assumed to be at zero potential and the conducting strip is assumed to be at 1-V potential. The potential at point i (which may for instance be in the center of the ith subsection) may be written as follows:

$$V_i = \sum_{j=1}^{n} \sigma_j D_{ij} = 1$$

(since the potential was assumed to be equal to unity on the rectangular pad), resulting in the matrix equation

$$[V] = [D][\sigma]. \tag{1}$$

The unknown charge densities $[\sigma]$ are obtained by matrix inversion:

$$[\sigma] = [D]^{-1}[V]. \tag{2}$$

The capacitance of the rectangular pad is

$$C = \sum_{j=1}^{n} \sigma_j = \sum_{i=1}^{n} \sum_{j=1}^{n} D_{ij}' \tag{3}$$

where D_{ij}' represents an element of matrix $[D]^{-1}$.

Fig. 2 shows the results of computation for the capacitance of rectangular sections of microstrip, for a range of aspect ratios L/W between 0.2 and 1.0, and for three different dielectric constants ($\epsilon_r = 1.0$, 6.0, 9.6). For $\epsilon_r = 1$, these results agree with Reitan [9] within 2 percent. A comparison has also been made with data for a dielectric-loaded parallel-plate capacitor by Adams and Mautz [10] for $\epsilon_r = 10$. This is a different but related problem. The data for the two problems agree within 5 percent for $H/W \leq 5.0$.

Clearly, the method described above may be applied to any three-dimensional N-port microstrip geometry of finite dimensions. For the N-port case, with small n total subsections, (1) is written as before except that N different voltages appear in matrix $[V]$. The capacitance coefficients and the direct-capacitance coefficients are calculated by partitioning $[D]^{-1}$ and summing the appropriate terms.

Our motivation for treating the rectangular section is related to discontinuity problems; the method used in all of the discontinuity problems is treated here.

B. Microstrip Discontinuities

1) The General Discontinuity Problem: The general discontinuity problem is represented in Fig. 3. The discontinuity region is finite but is connected to one or more infinitely long microstrip transmission lines. We wish to describe the network properties of the discontinuity.

First, we determine the N-port direct-capacitance matrix of the finite structure with transmission lines each of arbitrary length L (see Fig. 3), with the ground plane as reference:

$$[C(L)] = \begin{bmatrix} C_{11}(L) & \cdots & C_{1N}(L) \\ \cdots & \cdots & \cdots \\ C_{N1}(L) & \cdots & C_{NN}(L) \end{bmatrix}. \tag{4}$$

The direct-capacitance matrix is determined by matrix methods as described in Section II-A of this paper.

The discontinuity may be represented by a lumped direct-capacitance matrix $[C]$, where

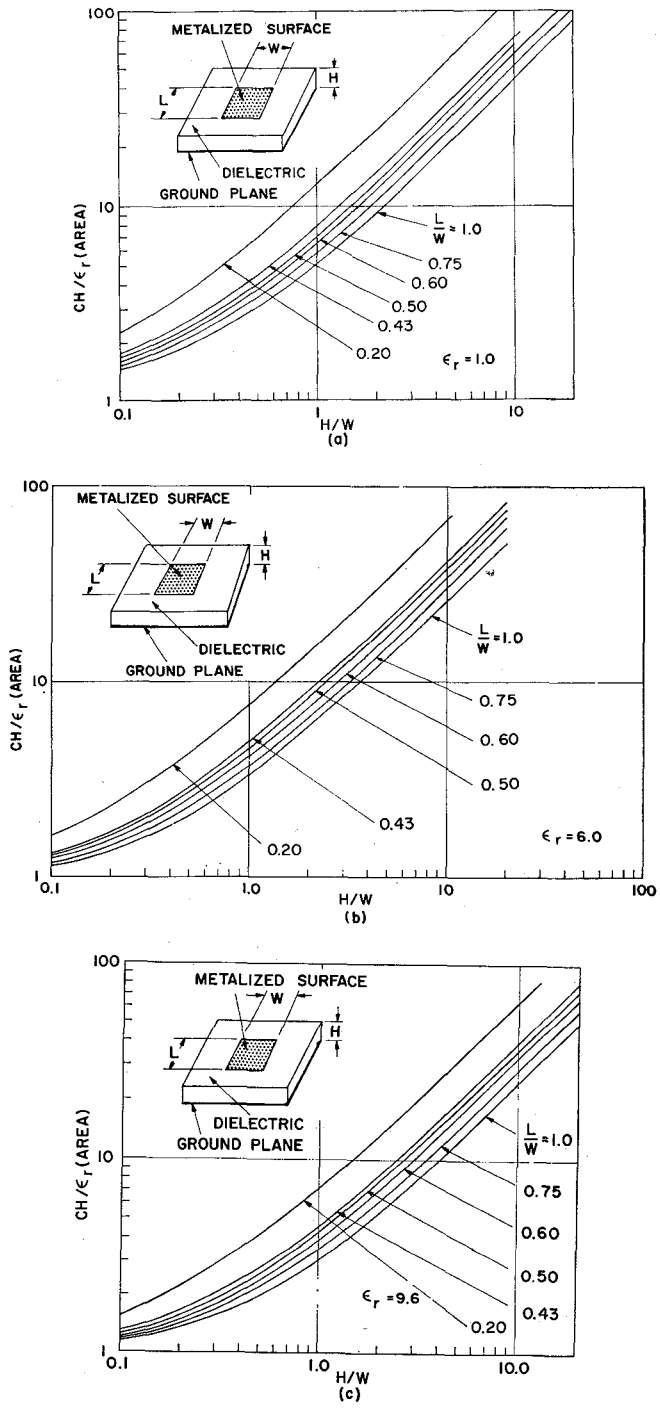

Fig. 2. Capacitances of microstrip rectangular sections.

$$[C] = \begin{bmatrix} C_{11} & C_{12} & \cdots & C_{1N} \\ C_{12} & C_{22} & \cdots & C_{2N} \\ \cdots & \cdots & \cdots & \cdots \\ C_{N1} & C_{N2} & \cdots & C_{NN} \end{bmatrix} \tag{5}$$

where

$$C_{ii} = \lim_{L \to \infty} [C_{ii}(L) - C_{oi}L - C_{oc(i)}] \tag{6}$$

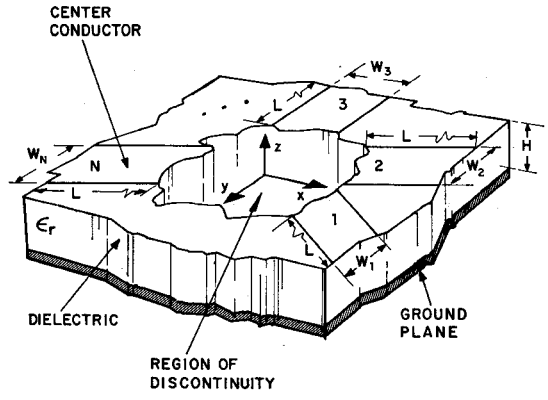

Fig. 3. A generalized microstrip discontinuity.

$$C_{ij} = \lim_{L\to\infty} C_{ij}(L), \qquad (i \neq j) \tag{7}$$

and where $C_{ij}(L)$ is the element of the direct-capacitance matrix for the finite structure, C_{oi} is the capacitance per unit length (two-dimensional capacitance) of the ith transmission line, and $C_{oc(i)}$ is the lumped open-circuit capacitance of the ith line.

Note that in deriving (5) from (4) we have assumed that the interactions between the infinite sections of transmission lines are negligible, i.e., we assume that most of the electric field lines between structure i and structure j remain within the discontinuity region. This is a good approximation in many cases. It would be a poor approximation if the transmission lines were closely spaced and parallel. In the parallel case, the effect of coupling can be taken directly into account in (5) by subtracting c_{oij} (two-dimensional capacitance per unit length). In any case, the matrix methods for the capacitance matrix yield the complete charge distribution and the distribution of flux lines between conductors so that these various effects can be separated out if necessary.

Note that we treat problems in which the capacitive effects predominate. Clearly, discontinuities involving significant inductive effects, such as bends and spirals, require an extension of the method.

2) Lumped Capacitance of Open-Circuited Microstrip: A semi-infinite open-circuited microstrip transmission line is shown in Fig. 4. Δ (see Fig. 4) is the distance from the end to the electrical open-circuit position. The effect of the discontinuity may be represented by a lumped shunt capacitance C_{oc}. C_{oc} is computed as follows: the total capacitance of a rectangular section for an arbitrary length L, such as is shown in Fig. 1, is computed. Then the length L is increased iteratively and the total capacitance $C_t(L)$ is computed every time. The equivalent circuit of the open-circuited line of finite length L may then be represented as in Fig. 5(a). We define $C_{exc}(L)$ as follows: $C_{exc}(L) = \frac{1}{2}[C_t(L) - C_oL]$, where C_o is the capacitance per unit length of the infinite (two-dimensional) line of dimensions W and H and $C_t(L)$ is

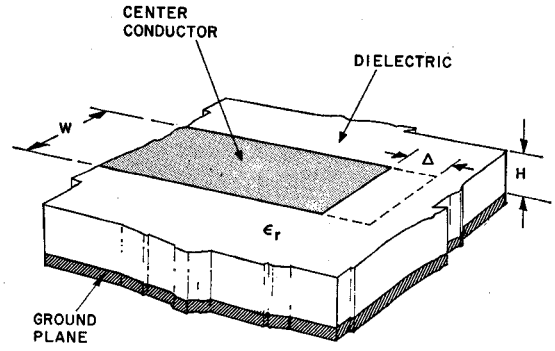

Fig. 4. Open-circuited microstrip.

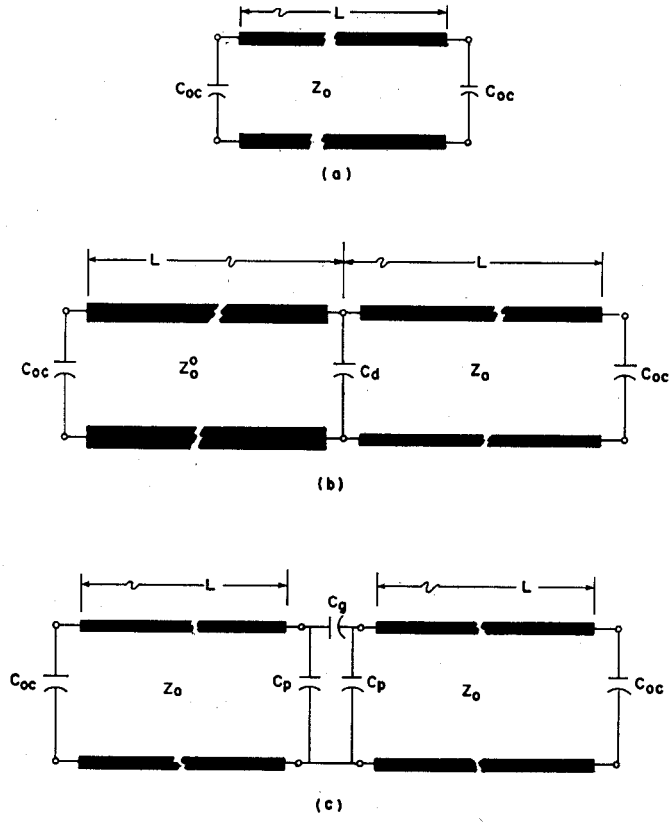

Fig. 5. Equivalent circuits for three microstrip discontinuities. (a) Open-circuited microstrip. (b) Sudden change of width. (c) Gap in microstrip.

the direct total capacitance of the open-circuited line with arbitrary length L. $2C_{exc}(L)$ thus represents the excess capacitance of the finite line, and as $L\to\infty$, $C_{exc}(L)\to C_{oc}$:

$$C_{oc} = \tfrac{1}{2} \lim_{L\to\infty} [C_t(L) - C_oL]. \tag{8}$$

There are several problems involved in such an iterative procedure. The infinite series in the three-dimensional source function converges rather slowly. The iterative procedure also converges slowly. Moreover, the procedure involves the subtraction of two nearly equal large numbers so that a very precise comparison of

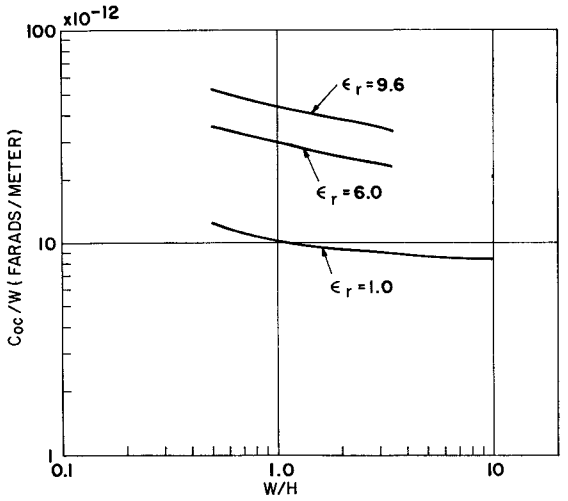

Fig. 6. Excess capacitances of open-circuited microstrip.

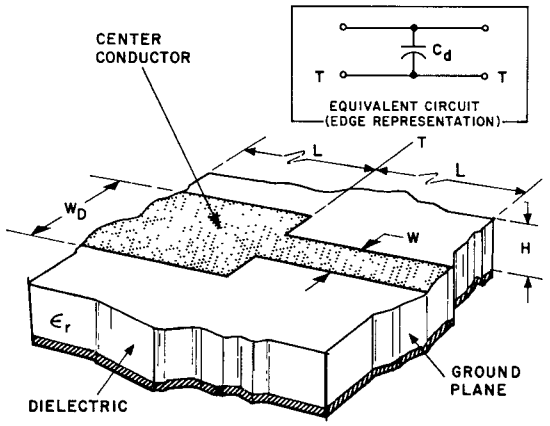

Fig. 7. Microstrip with sudden change of width.

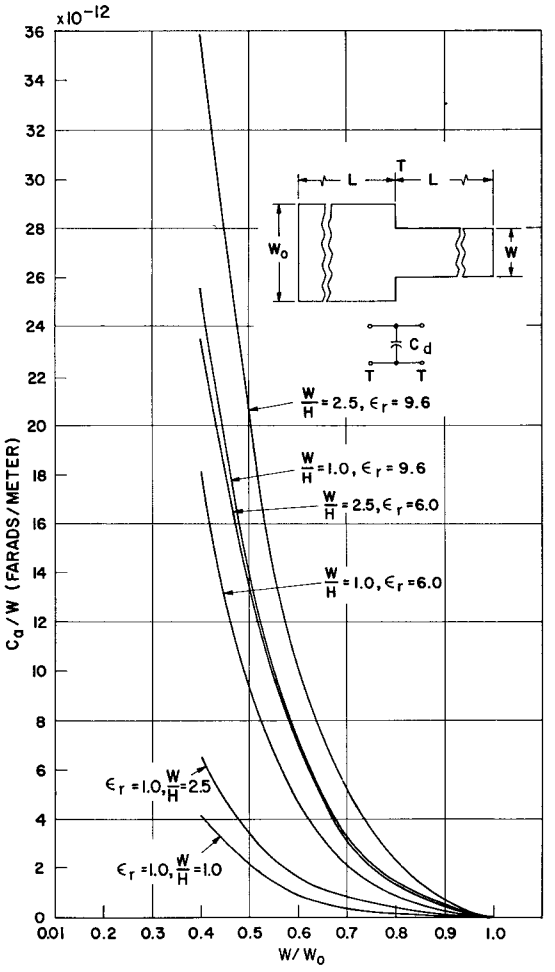

Fig. 8. Discontinuity capacitances for change of width in microstrip.

$C_t(L)$ and C_oL is necessary. A number of steps have been taken to improve the convergence. We take advantage of the fourfold symmetry of the geometry in open-circuited line. The length of the subsections was varied using very large subsections in the center of the section, where the charge density is most uniform. A geometric progression in the subsection lengths was used. The computation is still time-consuming; about 7 min of computer time are required for each open-circuit lumped-capacitance computation. Additional computational details are included in Section III.

Fig. 6 shows the normalized lumped capacitance C_{oc}/W of open-circuited microstrip for a range of aspect ratios W/H of 0.5 to 10 and for several dielectric constants ($\epsilon_r = 1.0$, 6.0, 9.6). The data for $\epsilon_r = 9.6$ have been compared with measured data with good agreement for $W/H \leq 1.0$. The open-circuit capacitance data are basic to the computation of the lumped-capacitance matrix of any discontinuity (6).

3) Sudden Change of Linewidth: Fig. 7 shows a microstrip transmission line in which the center conductor width is abruptly changed. The equivalent circuit for this problem consists of a shunt capacitance C_d and is also shown in Fig. 7.

To obtain C_d we consider a finite three-dimensional geometry consisting of two lines of widths W_o and W, respectively, each of length L. The equivalent circuit is shown in Fig. 5(b). The total capacitance $C_t(L)$ is computed. As $L \rightarrow \infty$ the discontinuity capacitance C_d may be expressed as

$$C_d = \lim_{L \rightarrow \infty} [C_t(L) - C_{oc}(1) - C_{oc}(2) - C_{o1}L - C_{o2}L] \quad (9)$$

where $C_{oc}(1)$ and $C_{oc}(2)$ are the open-circuit lumped capacitances of lines of width W_o and W, respectively, and C_{o1} and C_{o2} are the capacitances per unit length of the infinite (two-dimensional) lines of widths W_o and W, respectively.

Fig. 8 shows the results of computation for ratios W/W_o between 0.4 and 1.0 for several values of aspect ratio W/H and for several dielectric constants ($\epsilon_r = 1.0$, 6.0, 9.6).

4) Gap in Center Conductor: Fig. 9 shows a microstrip transmission line with a gap of length s. The equivalent circuit of the discontinuity may be represented as shown in Fig. 9. The discontinuity capacitance matrix is a symmetrical matrix of order two as shown by the equivalent circuit [Fig. 5(c)]. The elements of this matrix are determined as follows.

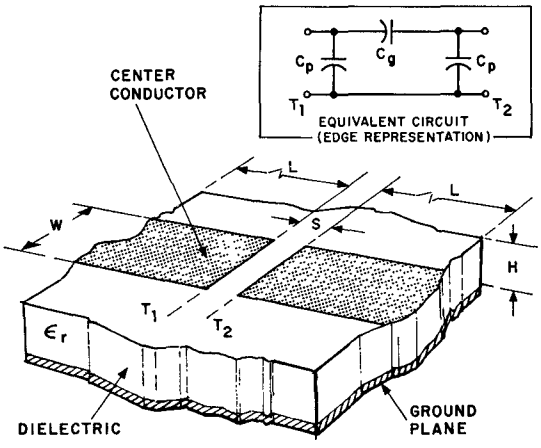

Fig. 9. Gap in microstrip.

We start with the geometry shown in Fig. 9 consisting of two lines of arbitrary length L separated by a gap. The equivalent circuit is shown in Fig. 5(c). We compute the capacitance matrix as a function of L and then obtain the matrix of the direct capacitances denoted by $[C(L)]$:

$$[C(L)] = \begin{bmatrix} C_{11}(L) & C_{12}(L) \\ C_{12}(L) & C_{11}(L) \end{bmatrix} \tag{10}$$

and

$$C_p = \lim_{L\to\infty} [C_{11}(L) - C_o L - C_{oc}]$$

$$C_g = \lim_{L\to\infty} C_{12}(L) = -\lim_{L\to\infty} c_{12}(L).$$

The computation of C_g does not involve the subtraction of nearly equal large numbers (as does the computation of C_p) and thus the computation of C_g is much less time-consuming.

Figs. 10 and 11 show the results of the computation of C_g and C_p, respectively, for various aspect ratios, separations, and dielectric constants. The data for C_g agree with those of Stinehelfer [6] to within 2 percent. For $\epsilon_r = 1$ the results were compared with Oliner [7], who has solved a related but different problem. For $W/H = 1$ and $\epsilon_r = 1.0$ the two results agree within 4 percent.

III. Computational Details

Symmetry was utilized to reduce the order of matrices and thus save computation time and memory requirements. The twofold symmetry of the change-of-linewidth problem and the fourfold symmetry in the open circuit, the gap problem, and the rectangular sections were taken into account. The computation time was reduced by about 40 percent through the use of the fourfold symmetry in the open-circuit problem. Of course, reducing the order of the matrix also helps to eliminate computational overflow and/or underflow.

The two-dimensional capacitances C_{o1} and C_{o2} of (9) and C_o of (8) were *not* computed directly from the two-dimensional formulation. Attempts to use the two-dimensional formulation resulted in very slow convergence of the iterative process. Instead we used the three-dimensional formulation [(11), in the Appendix] with single subsection along the length and multiple subsections along the width. As the strip becomes long (L/W, $L/H \gg 1$), the results of the two-dimensional and

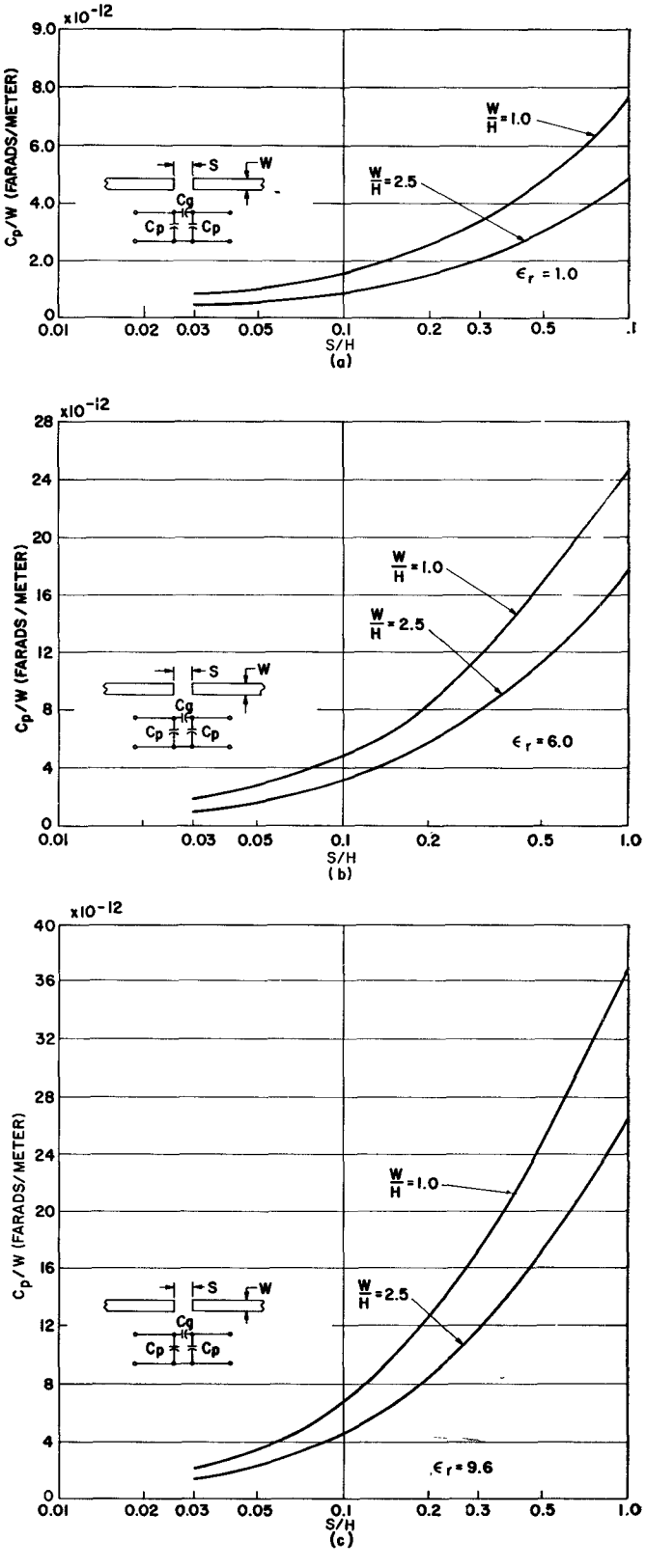

Fig. 10. Gap capacitance for gap discontinuity in microstrip.

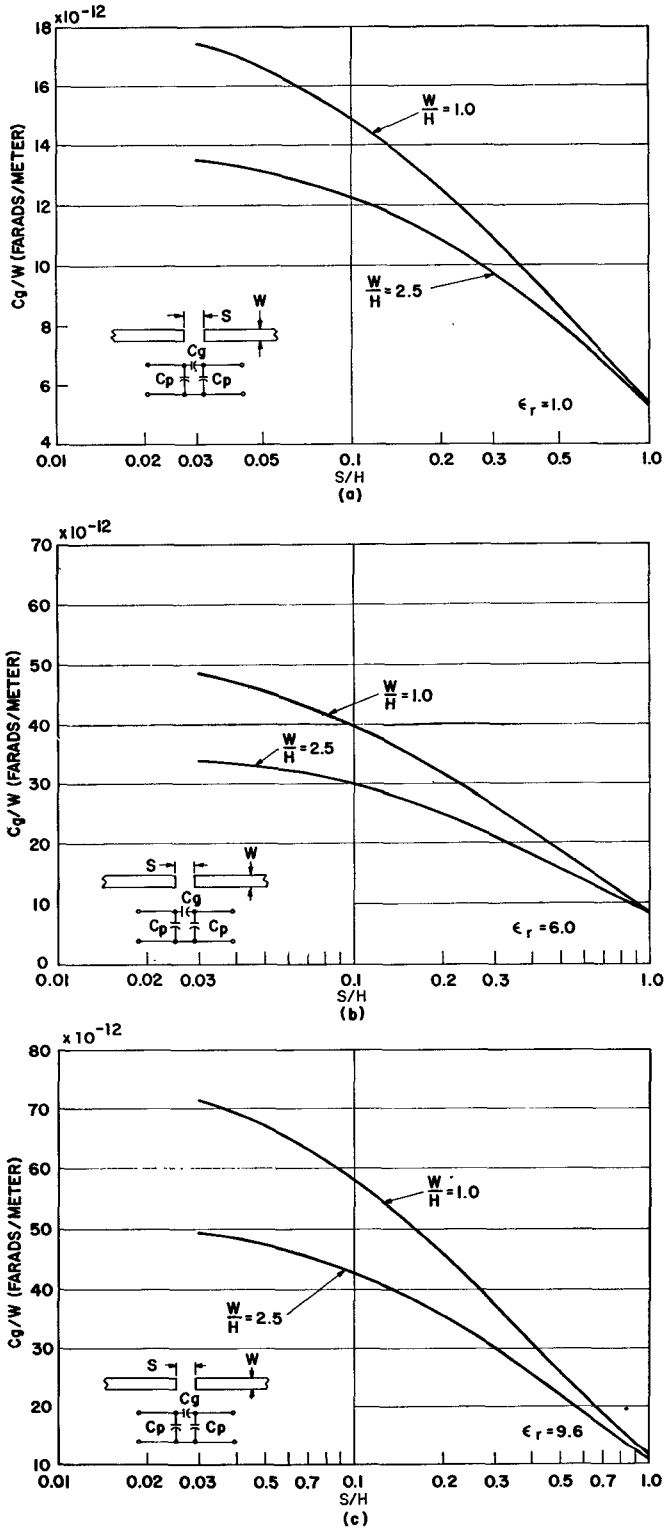

Fig. 11. Parallel capacitance for gap discontinuity in microstrip.

three-dimensional formulations agree closely (typically for four significant figures) and thus the use of this three-dimensional formulation is justified. Also, the final results show good agreement with experimental and theoretical data. The use of this three-dimensional formulation resulted in considerable improvement in the convergence of the iterative process. Apparently, this is due to the fact that we are computating $C_{ii}(L)$ and C_{oi} by a similar formulation.

In the computation of $C_{ii}(L)$, the number of subdivisions (n) increases through iteration. To maintain n within practical values, the length of the subsections was varied, with much longer subsections near the center of the transmission line where the charge density is nearly uniform. A geometric progression of subsection lengths was used. For example, in the computation of the open-circuit capacitance, 6 divisions along the width and 12 to 14 divisions along the length were sufficient.

Another factor in the computation time is the convergence of the infinite series in D_{ij}, (14). As noted earlier, the convergence of this series is slower than that of the two-dimensional source function. About 40 terms of the series were required in our three-dimensional computations as compared with about 10 terms required in the two-dimensional computations. As W/H decreases, the fringing becomes more important, and more terms of the series are required. It is estimated that our data are accurate within a few percent for $W/H \leq 1.0$; for wider strips the error may increase somewhat.

Total computation time for the capacitance data was about 1.8 min for each data point on rectangular sections, about 7 min for each open-circuit capacitance computation, about 18 min for each capacitance matrix for change of linewidth, and about 9 min for each capacitance matrix for the gap problem (GE635 computer was used in all computations). Considerable effort has been devoted to reducing computation time, but there are still several improvements that could be made. For instance, the block symmetry of the matrix (block Toeplitzicity) has not been utilized.

Impulsive weights (point matching) and pulse expansion functions [1] are used throughout. The matching point i is the center of subsection i.

IV. Conclusions

The matrix methods are applied to three-dimensional problems with emphasis upon the general problem of discontinuities in microstrip.

The discontinuities considered are: gap in microstrip, sudden change of width, and end effect. The data for the end effect are basic and enter into the computation of the lumped-capacitance matrix of other discontinuities. The method, as described, applies to those discontinuities in which capacitive effects predominate.

Computed data agree well with experiment and other data reported in the literature [6], [7], [9]. It is estimated that the results are accurate to within a few percent for $W/H < 1.0$.

Appendix
Three-Dimensional Source Function Potential of a Uniformly Charged Microstrip Subsection

Fig. 1 shows a rectangular section of microstrip divided into subsections. The typical subsection Δs_j of width Δx_j, length Δy_j, and center point (x_j, y_j, z_j) is shown.

The typical subsection lies in the plane $z=z_j$ with sides parallel to the x and y axes, respectively. It is assumed that the subsection is uniformly charged with surface charge density of magnitude unity. We wish to calculate the potential $V(x_i, y_i, z_i)$ at a field point (x_i, y_i, z_i), due to the uniformly charged typical subsection Δs_j.

First of all, we require the potential due to a uniformly charged plate in free space. Consider a uniformly charged rectangular plate identical to the subsection Δs_j shown in Fig. 1 and at an identical location in free space. Then the potential at a field point (x_i, y_i, z_i) is

$$V(x_i, y_i, z_i) = \frac{1}{4\pi\epsilon_o} \cdot \int_{x_1}^{x_2} \int_{y_1}^{y_2} \frac{dx'dy'}{\sqrt{(x_i - x')^2 + (y_i - y')^2 + (z_i - z')^2}} \tag{11}$$

where

$$x_1 = x_j - \frac{\Delta x_j}{2} \qquad y_1 = y_j - \frac{\Delta y_j}{2}$$

$$x_2 = x_j + \frac{\Delta x_j}{2} \qquad y_2 = y_j + \frac{\Delta y_j}{2}.$$

Integration yields the following result:

$$\begin{aligned} V(x_i, y_i, z_i) = \frac{1}{4\pi\epsilon_o} \Bigg\{ & (x_j - x_i) \log \frac{(c + A')(d + B')}{(d + C')(c + D')} \\ & + \frac{\Delta x_j}{2} \log \frac{(d + B')(d + C')}{(c + D')(c + A')} \\ & + (y_j - y_i) \log \frac{(a + A')(b + B')}{(b + D')(a + C')} \\ & + \frac{\Delta y_j}{2} \log \frac{(b + B')(b + D')}{(a + C')(a + A')} \\ & - h\left(\tan^{-1}\frac{ac}{hA'} + \tan^{-1}\frac{bd}{hB'}\right) \\ & + h\left(\tan^{-1}\frac{ac}{hC'} + \tan^{-1}\frac{bd}{hD'}\right)\Bigg\} \end{aligned} \tag{12}$$

where

$$a = x_j - \frac{\Delta x_j}{2} - x_i \qquad b = x_j + \frac{\Delta x_j}{2} - x_i$$

$$c = y_j - \frac{\Delta y_j}{2} - y_i \qquad d = y_j + \frac{\Delta y_j}{2} - y_i$$

$$A' = \sqrt{a^2 + c^2 + h^2} \qquad B' = \sqrt{b^2 + d^2 + h^2}$$

$$C' = \sqrt{a^2 + d^2 + h^2} \qquad D' = \sqrt{b^2 + c^2 + h^2}$$

$$h = z_j - z_i.$$

This result can also be obtained by summing the result given by Durand [11] for the potential over one corner of a uniformly charged rectangular plate. The potentials for four different rectangles are combined to obtain the final general result given in (12).

Now, we can treat the inhomogeneous problem of Fig. 1. The source function D_{ij} for the rectangular subsection of microstrip shown in Fig. 1 is obtained from the free-space source function by multiple imaging as follows [12], [13]:

$$D_{ij} = \sum_{n=1}^{\infty} a_n d_{ijn}(\text{above}) - a_n d_{ijn}(\text{below}) \tag{13}$$

where d_{ijn}(above) is the free-space source function for the nth image above the ground plane, d_{ijn}(below) is the free-space source function for the nth image below the ground plane, and a_n is the magnitude of the nth imaged charge given by

$$a_n = \frac{(-1)^{n+1}k^{n-1}2\epsilon}{(\epsilon + \epsilon_o)}.$$

d_{ijn}(above) and d_{ijn}(below) may be obtained from (12) by setting h equal to $(2n-2)H$ and $2nH$, respectively, and replacing ϵ_o with ϵ. Then, substituting d_{ijn}(above) and d_{ijn}(below) in (13) we obtain

$$\begin{aligned} D_{ij} = \sum_{n=1}^{\infty} \frac{(-1)^{n+1}k^{n-1}}{2\pi(\epsilon + \epsilon_o)} \cdot \Bigg\{ & (x_j - x_i) \log \frac{(c + A)(d + B)(d + G)(c + I)}{(d + C)(c + D)(c + E)(d + F)} \\ & + \frac{\Delta x_j}{2} \log \frac{(d + B)(d + C)(c + E)(c + I)}{(c + D)(c + A)(d + G)(d + F)} \\ & + (y_j - y_i) \log \frac{(a + A)(b + B)(b + I)(a + G)}{(b + D)(a + C)(a + E)(b + F)} \\ & + \frac{\Delta y_j}{2} \log \frac{(b + B)(b + D)(a + E)(a + G)}{(a + C)(a + A)(b + I)(b + F)} \\ & - (2n - 2)H\left(\tan^{-1}\frac{ac}{(2n - 2)HA} \right. \\ & \left. + \tan^{-1}\frac{bd}{(2n - 2)HB}\right) + (2n - 2)H \\ & \cdot \left(\tan^{-1}\frac{ad}{(2n - 2)HC} + \tan^{-1}\frac{bc}{(2n - 2)HD}\right) \\ & + 2nH\left(\tan^{-1}\frac{ac}{2nHE} + \tan^{-1}\frac{bd}{2nHF}\right) \\ & - 2nH\left(\tan^{-1}\frac{ad}{2nHG} + \tan^{-1}\frac{bc}{2nHI}\right)\Bigg\} \end{aligned} \tag{14}$$

where

$$A = \sqrt{a^2 + c^2 + (2n - 2)^2H^2} \qquad E = \sqrt{a^2 + c^2 + (2nH)^2}$$

$$B = \sqrt{b^2 + d^2 + (2n - 2)^2H^2} \qquad F = \sqrt{b^2 + d^2 + (2nH)^2}$$

$$C = \sqrt{a^2 + d^2 + (2n - 2)^2H^2} \qquad G = \sqrt{a^2 + d^2 + (2nH)^2}$$

$$D = \sqrt{b^2 + c^2 + (2n - 2)^2H^2} \qquad I = \sqrt{b^2 + c^2 + (2nH)^2}$$

and

$$k = \frac{\epsilon - \epsilon_o}{\epsilon + \epsilon_o}.$$

Acknowledgment

The authors would like to thank C. E. Nelson, General Electric Company, for helpful discussions, and G. Capraro, Rome Air Development Center, for his assistance in computation.

References

[1] R. F. Harrington, *Field Computation by Moment Methods*. New York: Macmillan, 1968.
[2] B. J. Strait and A. T. Adams, "Analysis and design of wire antennas with application to EMC," *IEEE Trans. Electromagn. Compat.*, vol. EMC-12, pp. 45–54, May 1970.
[3] R. F. Harrington, "Matrix methods for field problems," *Proc. IEEE*, vol. 55, pp. 136–149, Feb. 1967.
[4] A. Farrar and A. T. Adams, "Computation of lumped microstrip capacities by matrix methods—Rectangular sections and end effect," *IEEE Trans. Microwave Theory Tech.* (Corresp.), vol. MTT-19, pp. 495–497, May 1971.
[5] ——, "Computation of static capacitance data for single, double, and triple microstrip," in *1970 G-MTT Symp. Dig.*, pp. 257–261.
[6] H. Stinehelfer, "Strip transmission lines," *Microwave J.*, pp. 71–72, Feb. 1969.
[7] A. A. Oliner, "Equivalent circuit for discontinuities in balanced strip transmission line," *IRE Trans. Microwave Theory Tech. (Special Issue: Symposium on Microwave Strip Circuits)*, vol. MTT-3, pp. 134–143, Mar. 1955.
[8] J. R. Whinnery and H. W. Jamieson, "Equivalent circuit for discontinuities in transmission lines," *Proc. IRE*, vol. 32, pp. 98–114, Feb. 1944.
[9] D. K. Reitan, "Accurate determination of the capacitance of rectangular parallel plate capacitors," *J. Appl. Phys.*, vol. 30, no. 2, pp. 172–176, Feb. 1959.
[10] A. T. Adams and J. R. Mautz, "Computer solution of electrostatic problems by matrix inversion," in *Proc. 1969 Nat. Electronics Conf.*, pp. 198–201.
[11] E. Durand, *Electrostatique* I—*Les Distributions*. Paris, France: Masson et Cie, 1964, pp. 243–246.
[12] P. Silvester, "TEM wave properties of microstrip transmission line," *Proc. Inst. Elec. Eng.*, vol. 115, no. 1, pp. 43–48, Jan. 1968.
[13] Y. M. Hill, N. O. Reckord, and D. R. Winner, "A general method for obtaining impedance and coupling characteristics of practical microstrip and triplate transmission line configurations," *IBM J. Res. Develop.*, vol. 13, no. 3, pp. 314–322, May 1969.

Capacitance of Parallel Rectangular Plates Separated by a Dielectric Sheet

PETER BENEDEK, STUDENT MEMBER, IEEE, AND P. SILVESTER, MEMBER, IEEE

Abstract—**To determine the capacitance between two rectangular parallel plates separated by a dielectric sheet, the charge distribution on the plates is formulated in terms of a Fredholm integral equation of the first kind. This equation is solved numerically by a projective method using polynomial approximants. The resulting capacitance values are given in normalized graphical form, permitting capacitance determination for any practical values of dielectric constant and geometric parameters to within a few percent.**

Introduction

IN RECENT YEARS a substantial amount of literature has become available for microstriplike and related structures. But even with the increased use of integrated circuits, there appears to be very little data for finite plates on dielectric substrates. Reitan [1] obtained the capacitance of two parallel square plates *in vacuo* using the method of subareas. Harrington [2] solved the same problem using a closely related projection method. Adams and Mautz [3] found the capacitance of a rectangular dielectric loaded capacitor by the point-matching method and introduced special matrix elements to take care of the air–dielectric interface. Farrar and Adams [4] obtained, very recently, the capacitance of a rectangular section of a microstrip line by the method of moments with pulse-expansion functions and impulsive weights. They calculate the potential due to a uniformly charged rectangular plate *in vacuo* and then generate the Green's function as an infinite series of images.

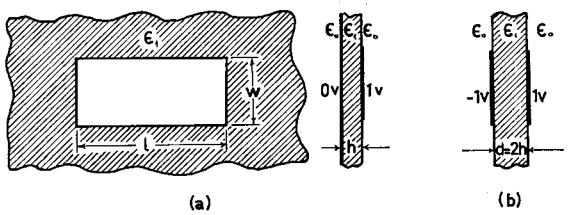

Fig. 1. (a) Rectangular metal plate on a metal-backed dielectric substrate. (b) Parallel plate problem, equivalent to (a).

This paper takes a different approach to the static capacitance for rectangular thin plates on a metal-backed dielectric substrate, as shown in Fig. 1(a). To facilitate the analysis, the equivalent problem, shown in Fig. 1(b), is considered. It is well known that the electrostatic behavior of this configuration is governed by Poisson's equation subject to Dirichlet boundary condi-

Manuscript received August 3, 1971; revised November 29, 1971. This work was supported in part by the Communications Research Centre and by the National Research Council of Canada.

The authors are with the Department of Electrical Engineering, McGill University, Montreal, Que., Canada.